JMB

The Cellulose-binding Domains from *Cellulomonas fimi* β-1,4-Glucanase CenC Bind Nitroxide Spin-labeled Cellooligosaccharides in Multiple Orientations

Philip E. Johnson, Emmanuel Brun, Lloyd F. MacKenzie, Stephen G. Withers and Lawrence P. McIntosh*

Protein Engineering Network of Centres of Excellence and Department of Chemistry and Department of Biochemistry and Molecular Biology University of British Columbia Vancouver, British Columbia V6T 1Z3, Canada

The N-terminal cellulose-binding domains CBD_{N1} and CBD_{N2} from *Cellulomonas fimi* cellulase CenC each adopt a jelly-roll β-sandwich structure with a cleft into which amorphous cellulose and soluble cellooligosaccharides bind. To determine the orientation of the sugar chain within these binding clefts, the association of TEMPO (2,2,6,6-tetramethylpiperidine-1-oxyl-4-yl) spin-labeled derivatives of cellotriose and cellotetraose with isolated CBD_{N1} and CBD_{N2} was studied using heteronuclear ^{1}H-^{15}N NMR spectroscopy. Quantitative binding measurements indicate that the TEMPO moiety does not significantly perturb the affinity of the cellooligo-saccharide derivatives for the CBDs. The paramagnetic enhancements of the amide ^{1}H^N longitudinal (ΔR_1) and transverse (ΔR_2) relaxation rates were measured by comparing the effects of TEMPO-cellotetraose in its nitroxide (oxidized) and hydroxylamine (reduced) forms on the two CBDs. The bound spin-label affects most significantly the relaxation rates of amides located at both ends of the sugar-binding cleft of each CBD. Similar results are observed with TEMPO-cellotriose bound to CBD_{N1}. This demonstrates that the TEMPO-labeled cellooligosaccharides, and by inference strands of amorphous cellulose, can associate with CBD_{N1} and CBD_{N2} in either orientation across their β-sheet binding clefts. The ratio of the association constants for binding in each of these two orientations is estimated to be within a factor of five to tenfold. This finding is consistent with the approximate symmetry of the hydrogen-bonding groups on both the cellooligosaccharides and the residues forming the binding clefts of the CenC CBDs.

© 1999 Academic Press

Keywords: protein-carbohydrate interaction; NMR; spin label; glycosynthase

*Corresponding author

Introduction

The β-1,4-glucanase CenC from *Cellulomonas fimi* is modular in structure and function (Coutinho *et al.*, 1992, 1991). Its central catalytic domain is connected by a short linker to two tandem N-terminal cellulose-binding domains, CBD_{N1} and CBD_{N2}(Tomme *et al.*, 1995). In contrast to most CBDs which bind crystalline cellulose, the homologous family IV CBD_{N1} and CBD_{N2} from CenC are unique in their specificity for amorphous cellulose and soluble cellooligosaccharides. As part of a col-

laborative effort to exploit these domains for use in biotechnology, we have used NMR spectroscopy and calorimetry to provide a structural and thermodynamic foundation for understanding the distinct binding properties of CBD_{N1} and CBD_{N2} (Creagh *et al.*, 1998; Johnson *et al.*, 1996a,b, 1998; Tomme *et al.*, 1996a).

CBD_{N1} (Johnson *et al.*, 1996b) and CBD_{N2} are composed of two five-stranded antiparallel (E.B., P.E.J. & L.P.M., unpublished results) β-sheets that fold into very similar jelly-roll sandwich structures. As demonstrated by NMR chemical shift perturbations and the observation of intermolecular protein-sugar NOEs, a single cellooligosaccharide molecule binds to these CBDs within a groove or cleft that runs across one β-sheet face of each protein domain (Johnson *et al.*, 1996a,b). The presence of a cleft readily explains the binding specificity of these CBDs. Soluble cellooligosaccharides and single polysaccharide chains, as might be encountered in the amorphous regions of cellulose, bind within this cleft, whereas flat crystalline arrays of cellulose are excluded. In agreement with the observation that the affinity of CBD_{N1} for cellooligosaccharides increases in the order cellotriose < cellotetraose < cellopentaose ∼ cellohexaose, the sugar binding sites in the CenC CBDs can each be spanned by approximately five glycosyl units (Johnson *et al.*, 1996a,b; Tomme *et al.*, 1996a).

In parallel with these structural studies, a detailed calorimetric analysis of the association of CBD_{N1} with polysaccharides was also conducted (Creach *et al.*, 1998; Tomme *et al.*, 1996a). CBD_{N1} was found to bind regenerated (phosphoric acid swollen) cellulose and other soluble β-1,4-linked polymers of glucose, such as hydroxyethyl cellulose and barley and oat-β-glucan, with affinities equal to those measured for cellopentaose and cellohexaose. Formation of the CBD_{N1}-sugar complexes is favored enthalpically, indicating that hydrogen bonding and van der Waals interactions provide the primary driving force for the binding event. Inspection of the structures of CBD_{N1} and CBD_{N2} reveals that their binding clefts consist of a central strip of hydrophobic side-chains, flanked on both sides by polar residues. This led us to propose that the pyranose rings of cellooligosaccharides, and by inference single polysaccharide chains in regions of amorphous cellulose, are stacked against the hydrophobic strip, while the flanking hydrophilic residues provide hydrogen bonds to the equatorial hydroxyl groups of the sugar (Johnson *et al.*, 1996a,b). Such interactions are often observed with carbohydrate-binding proteins (Quiocho, 1989, 1993; Vyas, 1991).

The structures of CBD_{N1} and CBD_{N2} were calculated using NMR data collected for these protein domains in the presence of saturating concentrations of cellotetraose or cellopentaose, respectively (Johnson *et al.*, 1996b). Numerous intermolecular nuclear Overhauser effects (NOEs) between the $^{13}C/^{15}N$-labeled proteins and the unlabeled cellooligosaccharides were observed in isotope edited/filtered NOESY experiments (Otting & Wüthrich, 1990). However, the NMR spectra of the cellooligosaccharides are highly degenerate, thus preventing the unambiguous assignment of these NOEs to specific interactions between sugar and protein protons. This precluded the direct determination of the structures of the CBD-cellooligosaccharide complexes.

As a first step towards achieving this goal, we have focussed on defining the orientation of a cellulose chain within the binding clefts of CBD_{N1} and CBD_{N2}. Exploiting a novel glycosynthase technology (Mackenzie *et al.*, 1998), we have prepared derivatives of cellotriose and cellotetraose with a 2,2,6,6-tetramethylpiperidine-1-oxy-4-yl (TEMPO) spin-label covalently attached to the reducing end of the sugar (Figure 1). The use of such paramagnetic relaxation probes has a long history in the study of biological macromolecules by NMR spectroscopy (Kosen, 1989). The nitroxide moiety contains an unpaired electron that provides an efficient mechanism for the relaxation of neighboring nuclei *via* dipolar coupling. Due to the magnitude of the electron magnetic moment, this interaction extends to over 20 Å. In contrast, proton-proton NOEs are limited to separations of less than ∼5 Å. Thus, these TEMPO-labeled sugars can be utilized to obtain long-range distance information about the CBD-cellooligosaccharide complexes. In practice, the excellent dispersion of the signals from the amide ^1H-^{15}N groups, combined with the high degree of sensitivity of the HSQC experiment (Cavanagh *et al.*, 1996), allows the effect of the spin-label cellooligosaccharides on
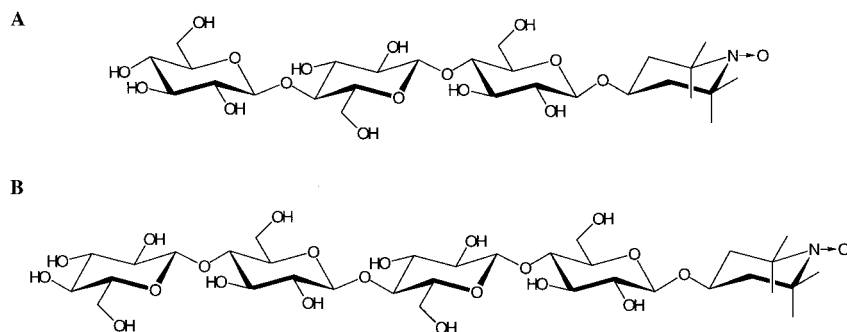

Figure 1. Chemical structures of the spin-labeled glycosides: (a) TEMPO-Glc$_3$ and (b) TEMPO-Glc$_4$. Reduction of the paramagnetic nitroxide (N-O) moiety produces the diamagnetic hydroxylamine (N-OH) derivatives of these glycosides.

each non-proline residue in ^{15}N-labeled CenC CBDs to be evaluated. Similar studies using spin-labeled ligands and heteronuclear NMR methods have been reported by several groups (Gellespie & Shortle, 1997a,b; Zhao et al., 1997; Kleerekoper et al., 1995; Yu et al., 1994). Using this approach, we demonstrate that the modified sugars bind to CBD$_{N1}$ and CBD$_{N2}$ in both possible orientations across their β-sheet binding clefts. This result is consistent with the approximate symmetry of the cellooligosaccharides and the positions of the side-chains forming the binding clefts of the two protein domains, as well as ^{15}N relaxation measurements which indicate that residues within the binding cleft of CBD$_{N1}$ remain conformationally flexible in the presence of these sugars (P.E.J., E.B. & L.P.M., unpublished results).

Results

Preparation of TEMPO-labeled cellooligosaccharides

Syntheses of the nitroxide spin-labeled cellotrio-side (TEMPO-Glc$_3$) and cellotetraoside (TEMPO-Glc$_4$) were accomplished in a two-step chemo-enzymatic process, thereby avoiding many of the difficulties inherent in the preparation of oligosaccharide derivatives by chemical methods alone. A TEMPO-labeled glucoside was first synthesized via standard Koenigs-Knorr methodology, essentially according to a published procedure (Gnewuch & Sosnovsky, 1986; Plessas & Goldstein, 1981). This product was characterized by mass and, to a limited extent, ^{1}H-NMR spectroscopy. Full NMR spectroscopic characterization was performed on the catalytically hydrogenated (reduced) and acetylated hydroxylamine derivative that no longer bears a free radical. Conversion of the TEMPO-glucoside to TEMPO-Glc$_3$ and Glc$_4$ was accomplished by successive transfer of glucose residues from α-glucosyl fluoride using a mutant Agrobacterium sp. β-glucosidase (glycosynthase) in which the catalytic nucleophile, Glu358, was replaced by an alanine residue (Mackenzie et al., 1998). This approach exploits the well-known transglycosylation reaction catalyzed by retaining glycosidases, yet has the advantage that the mutant enzyme cannot hydrolyze the end products, thereby resulting in good yields of ~70% per coupling. The products were purified by HPLC and their identities confirmed by ionspray mass spectrometry, and after reduction and acetylation, by ^{1}H-NMR spectroscopy.

Binding of TEMPO-labeled cellooligosaccharides to CBD$_{N1}$ and CBD$_{N2}$

We have demonstrated previously, using NMR spectroscopy and isothermal titration calorimetry, that the monomeric CBD$_{N1}$ binds soluble cellooligosaccharides with a stoichiometry of 1:1 (Johnson et al., 1996a; Tomme et al., 1996a). Similar results
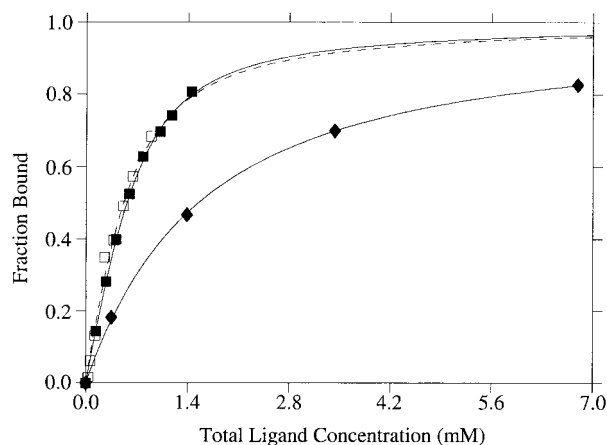

Figure 2. The association constants of the CenC CBDs for TEMPO-labeled cellooligosaccharides were measured using ^{1}H-^{15}N NMR spectroscopy. Shown are the normalized chemical shifts changes, or fraction bound, of the amide proton of Asn81 in CBD$_{N1}$ upon titration with TEMPO-Glc$_3$ (filled diamonds) and TEMPO-Glc$_4$ (filled squares), and the nitrogen atom of Val197 in CBD$_{N2}$ upon addition of TEMPO-Glc$_4$ (open squares). The solid and broken lines represent the best fits of the data to the Langmuir isotherm describing the binding of one ligand to a single protein site on CBD$_{N1}$ or CBD$_{N2}$, respectively. The total chemical shift changes for Asn81 and Val197 were extrapolated to be 0.1 ppm (^{1}H^N) and 0.76 ppm (^{15}N), respectively.

have been obtained with CBD$_{N2}$ (data not shown). Continuing this approach, the interactions of the TEMPO-labeled cellooligosaccharides with CBD$_{N1}$ and CBD$_{N2}$ were analyzed quantitatively by monitoring the ^{1}H^N and ^{15}N chemical shifts of the proteins upon titration with these soluble sugars. The spectral changes resulting from the addition of TEMPO-Glc$_3$ and TEMPO-Glc$_4$ are similar to those observed with the corresponding unlabeled cellooligosaccharides, indicating that these ligands all bind in the regime of fast exchange on the chemical shift timescale to the same regions in CBD$_{N1}$ and CBD$_{N2}$ and with the same 1:1 stoichiometry (data not shown). Apparent or macroscopic equilibrium association constants were obtained by fitting the titration data to the Langmuir isotherm describing the binding of one ligand molecule to a single protein site (Figure 2).

TEMPO-Glc$_3$ binds to CBD$_{N1}$ with an apparent K_a of 690($\pm$260) M^{-1}. This is marginally higher than the value of 180($\pm$60) M^{-1} measured previously for unlabeled cellotriose (Johnson et al., 1996a). The apparent K_a values of TEMPO-Glc$_4$ for CBD$_{N1}$ and CBD$_{N2}$ are 4200($\pm$400) M^{-1} and 3600($\pm$2200) M^{-1}, respectively, while the association constants of CBD$_{N1}$ and CBD$_{N2}$ for unlabeled cellotetraose are 4200($\pm$720) M^{-1} (Johnson et al., 1996a) and 7000($\pm$650) M^{-1} (data not shown). The relatively large errors in the K_a values measured for the TEMPO-labeled cellooligosaccharides reflect the fact that the nitroxide efficiently broadens the

signals from many amide groups within the binding cleft to the point that they are no longer observable. In general, it is these amide groups that show the largest chemical shift changes upon addition of sugar to the protein and would otherwise be best suited for fitting to the binding isotherm equation. Within the error of the data, we conclude that the TEMPO moiety does not significantly perturb the affinity of the CenC CBDs for these cellooligosaccharides. By way of comparison, increases in affinity of ~10 to 20-fold result from the lengthening of cellotriose or cellotetraose by one additional glycosyl unit to form cellotetraose

or cellopentaose, respectively (Tomme *et al.*, 1996a).

TEMPO-labeled cellooligosaccharides bind CBD$_{N1}$ and CBD$_{N2}$ in multiple orientations

In addition to perturbing the chemical shifts of amide groups in CBD$_{N1}$ and CBD$_{N2}$, the binding of TEMPO-Glc$_3$ and Glc$_4$ causes a decrease in the intensities of the signals from many of these groups due to paramagnetic relaxation enhancement. This is readily seen by comparing the ^{1}H-^{15}N HSQC spectra of two proteins complexed with the oxidized and reduced cellotetraose derivative
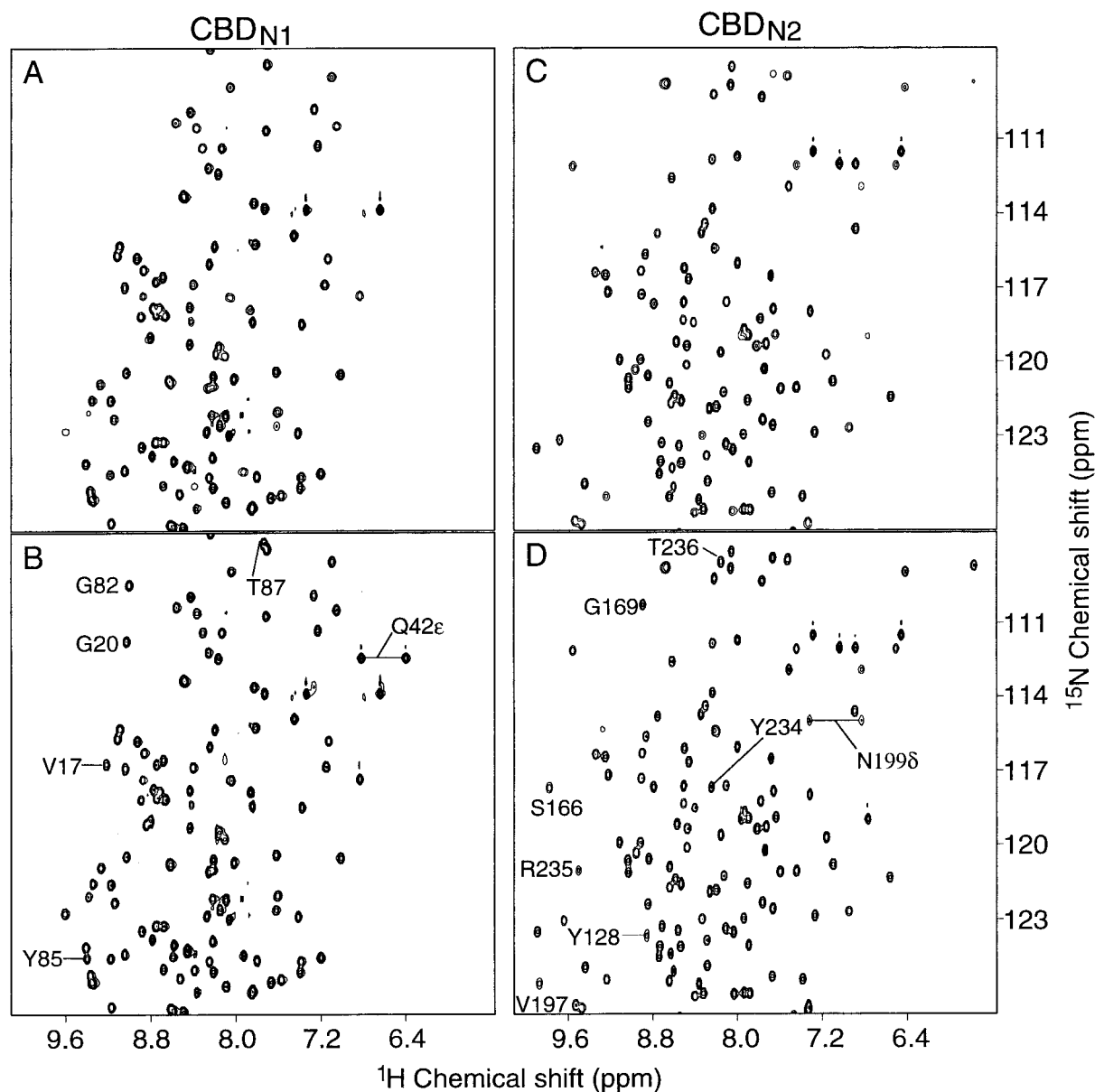
Figure 3. Portions of the non-sensitivity enhanced ^{1}H-^{15}N HSQC spectra of (a), (b) CBD$_{N1}$ and (c), (d) CBD$_{N2}$ bound to (a), (c) oxidized or (b), (d) reduced TEMPO-Glc$_4$. The final ligand-to-protein ratios of 2.2:1 and 1.4:1 correspond to ~80% and 65% saturation of CBD$_{N1}$ and CBD$_{N2}$, respectively. Peaks from amides that "disappear" because of paramagnetic relaxation due to the nearby unpaired electron in the nitroxide-labeled cellotetraose are identified.

(Figure 3). Qualitatively, it is clear that a number of resonances present in the spectra of proteins bound to the reduced hydroxylamine form of the sugar are "absent" in the spectra recorded with the oxidized nitroxide form, i.e. their intensities fall below a very low contour level. Thus, these amide groups must be close ($\leqslant 11$ Å; *vide infra*) to the free electron in the nitroxide moiety.

The amide protons whose resonances are absent in the ^{1}H-^{15}N HSQC spectra of the complexes of TEMPO-Glc$_4$ with CBD$_{N1}$ and CBD$_{N2}$ can be classified into two groups that are located on the opposite ends of the binding clefts of these proteins. (As shown in Figure 5, the binding cleft of each CBD lies across an antiparallel β-sheet A formed by five strands, arranged as A1-A2-A5-A3-A4.) In the case of CBD$_{N1}$, the first group includes Val17, Ala18, Tyr19 and Gly20 from β-strand A1, while the second group comprises Tyr85, Gly86 and Thr87 from β-strand A4 and the loop between A3 and A4. Similarly, for CBD$_{N2}$, the first group is formed by Ser166, Leu167, Tyr168, Gly169 from β-strand A1, while the second group includes of Tyr234, Arg235 and Thr236 from β-strand A4 and the preceding loop. In contrast, peaks from amide protons in the central β-strand A5 of each CBD are present in the ^{1}H-^{15}N HSQC spectra. Inspection of the tertiary structures of CBD$_{N1}$ and CBD$_{N2}$ reveals that the outermost strands, A1 and A4, are separated by ~20 Å. The observation that the amide protons, which are most strongly perturbed by the nitroxide spin label, are located in both of these outer β-strands cannot be accounted for by the binding of TEMPO-Glc$_4$ to the CBDs in a single orientation. The simplest explanation of this result is that TEMPO-Glc$_4$ associates with CBD$_{N1}$ and CBD$_{N2}$ in at least two distinct orientations, such that the nitroxide moiety lies at either edge of their sugar binding clefts.

The peaks from amide protons in β-strands A1 and A4 that are absent in the spectrum of CBD$_{N1}$ bound to TEMPO-Glc$_4$ also disappear upon binding TEMPO-Glc$_3$ (see Supplementary Material). In addition, signals from several amide protons, including those of Thr21 in strand A1 and Ala41, Gln42$^\varepsilon$, Tyr43, Val48, Asn50, and Gly51 in strand A2, are weak in the spectrum of CBD$_{N1}$ complexed with TEMPO-Glc$_4$ and absent in the presence of TEMPO-Glc$_3$. This qualitative distinction may reflect a slight difference in the positions of the two sugars when bound to CBD$_{N1}$. Several protons, including the indole H$^{\varepsilon1}$ of Trp16 and the amide H^N of Leu146, which are not in the binding cleft of CBD$_{N1}$, are also affected by TEMPO-Glc$_3$. This is attributed to non-specific effects arising from the addition of a 22-fold molar excess of the nitroxide-labeled sugar to the protein sample.

Measurement of ΔR_1 and ΔR_2 relaxation enhancements

A qualitative inspection of the ^{1}H-^{15}N HSQC spectra of the two CBD-TEMPO-Glc$_4$ complexes provides immediate insights into the binding orientations of the sugars. Further details regarding the positions of the bound nitroxide moiety can be gained by a quantitative analysis of the effects of the spin label on the relaxation properties of the two CBDs. To reduce the possibility of non-specific interactions, CBD$_{N1}$ and CBD$_{N2}$ were studied at saturation levels of approximately 80% and 65%, respectively (Figure 2).

The enhancements of the longitudinal (ΔR_1) and transverse (ΔR_2) relaxation rates of CBD$_{N1}$ and CBD$_{N2}$ due to complexation with TEMPO-Glc$_4$ are presented in Figures 4 and 5. Data for CBD$_{N1}$ bound to TEMPO-Glc$_3$ are provided as Supplementary Material. The ΔR_1 values were determined from the differences in the T_1 lifetimes, measured using a ^{1}H-^{15}N HSQC sequence as a read-out of a non-selective inversion-recovery sequence (Cavanagh *et al.*, 1996), for the proteins in the presence of the nitroxide and hydroxylamine derivatives of cellotetraose. The ΔR_2 values were obtained using two complementary methods. In the first, the effect of the spin label on the proton transverse relaxation ($\Delta R_{2,Vol}$) of the ^{1}H^N during the INEPT and reverse-INEPT period of the HSQC pulse sequence was measured by comparing the total volume of its cross-peak in spectra recorded with the oxidized and reduced sugar. In the second, $\Delta R_{2,LW}$ was determined from the change in the proton line-width of the amide measured with the two forms of the modified cellotetraose. The methods for determining ΔR_1 and ΔR_2 assume that contributions to the peak volumes and line-widths due to scalar couplings and relaxation processes other than that mediated by the free radical remain constant, and that the oxidized and reduced glycosides interact identically with the CBDs. The lack of any significant amide ^{1}H^N or ^{15}N chemical shift perturbation upon reduction of the TEMPO group provides strong support for these assumptions (Figure 3).

Following these approaches, 101 ΔR_1, 64 $\Delta R_{2,Vol}$, and 99 $\Delta R_{2,LW}$ values were obtained for CBD$_{N1}$ and 113 ΔR_1, 44 $\Delta R_{2,Vol}$, and 118 $\Delta R_{2,LW}$ values for CBD$_{N2}$ (Figure 4). Rate enhancements were not measurable for the remaining non-proline residues for two reasons, besides spectral overlap. First, in the case of those amide protons that are closest to the nitroxide moiety, severe line-broadening rendered their signals undetectable in the spectra recorded with oxidized TEMPO-Glc$_4$. For these residues, we estimate $\Delta R_1 > 2.5$ s^{-1} and $\Delta R_2 > 80$ s^{-1}. Second, in the case of those amide protons furthest from the nitroxide group, changes in their relaxation rates were too small to measure reliably. In particular, dilution effects due to the addition of ascorbic acid and subsequent pH adjustments caused the volumes of the peaks in the ^{1}H-^{15}N HSQC spectra of the proteins recorded with the reduced sugar to decrease slightly. This led to small apparent negative $\Delta R_{2,Vol}$ values for many
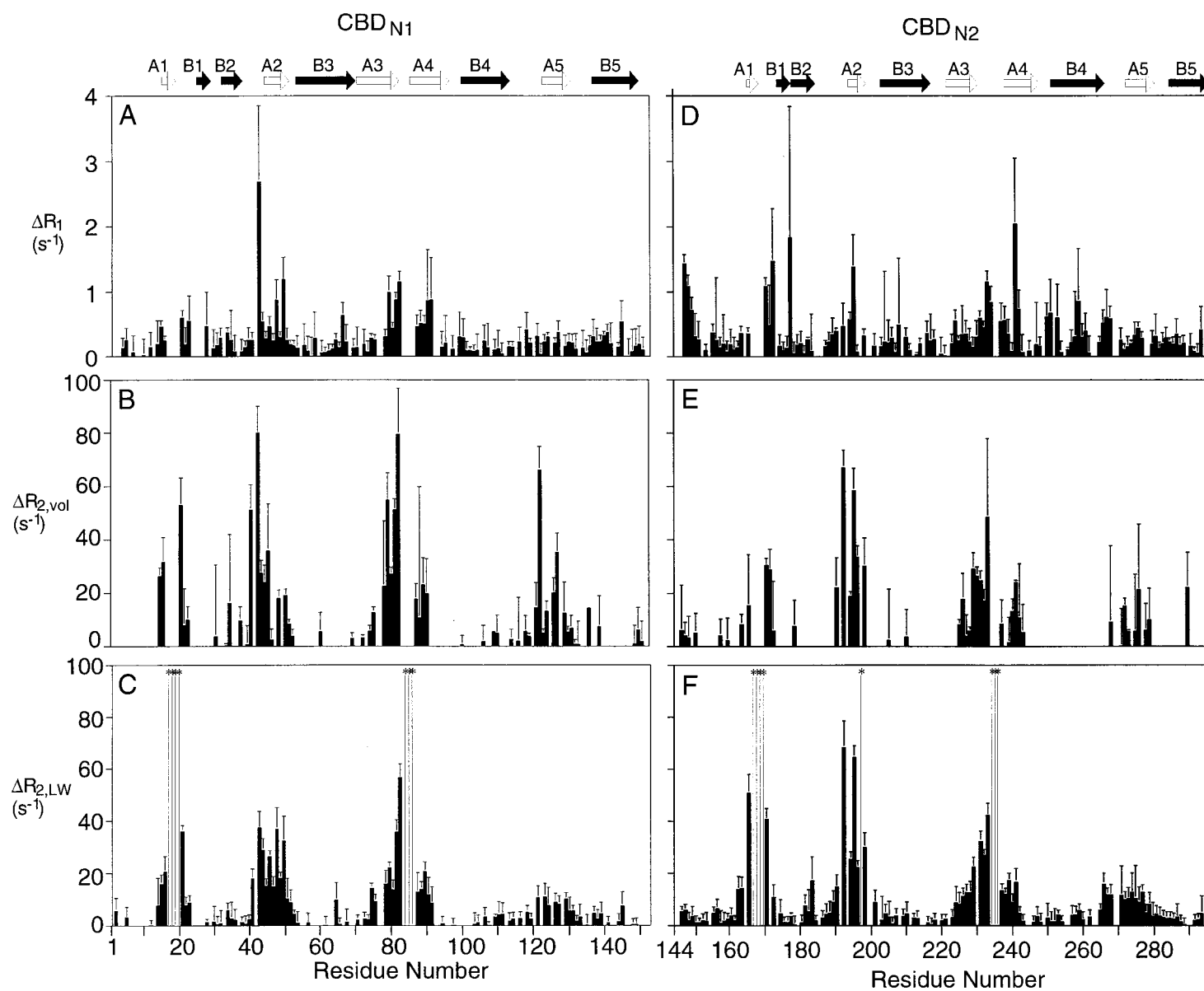
Figure 4. The enhancement of the amide $^1H^N$ longitudinal (ΔR_1) and transverse ($\Delta R_{2,Vol}$ and $\Delta R_{2,LW}$) rates resulting from the binding of TEMPO-Glc$_4$ by (a), (b), (c) CBD$_{N1}$ and (d), (e), (f) CBD$_{N2}$. Only positive rate enhancements are shown. Residues whose signals disappear completely due to the nitroxide spin label are identified in (c) and (f) with an asterisk. The locations of the β-strands forming sheets A and B in the two proteins are indicated by the open and filled arrows, respectively.

Figure 5. Paramagnetic relaxation studies demonstrate that TEMPO-Glc$_4$ binds to each CenC CBD in at least two orientations such that the nitroxide moiety can lie at either end of the binding cleft. Shown are ribbon diagrams of CBD$_{N1}$ (left) and CBD$_{N2}$ (right) positioned for the reader to look across (top) and down onto (bottom) the cellooligo-saccharide binding groove that is formed by β-s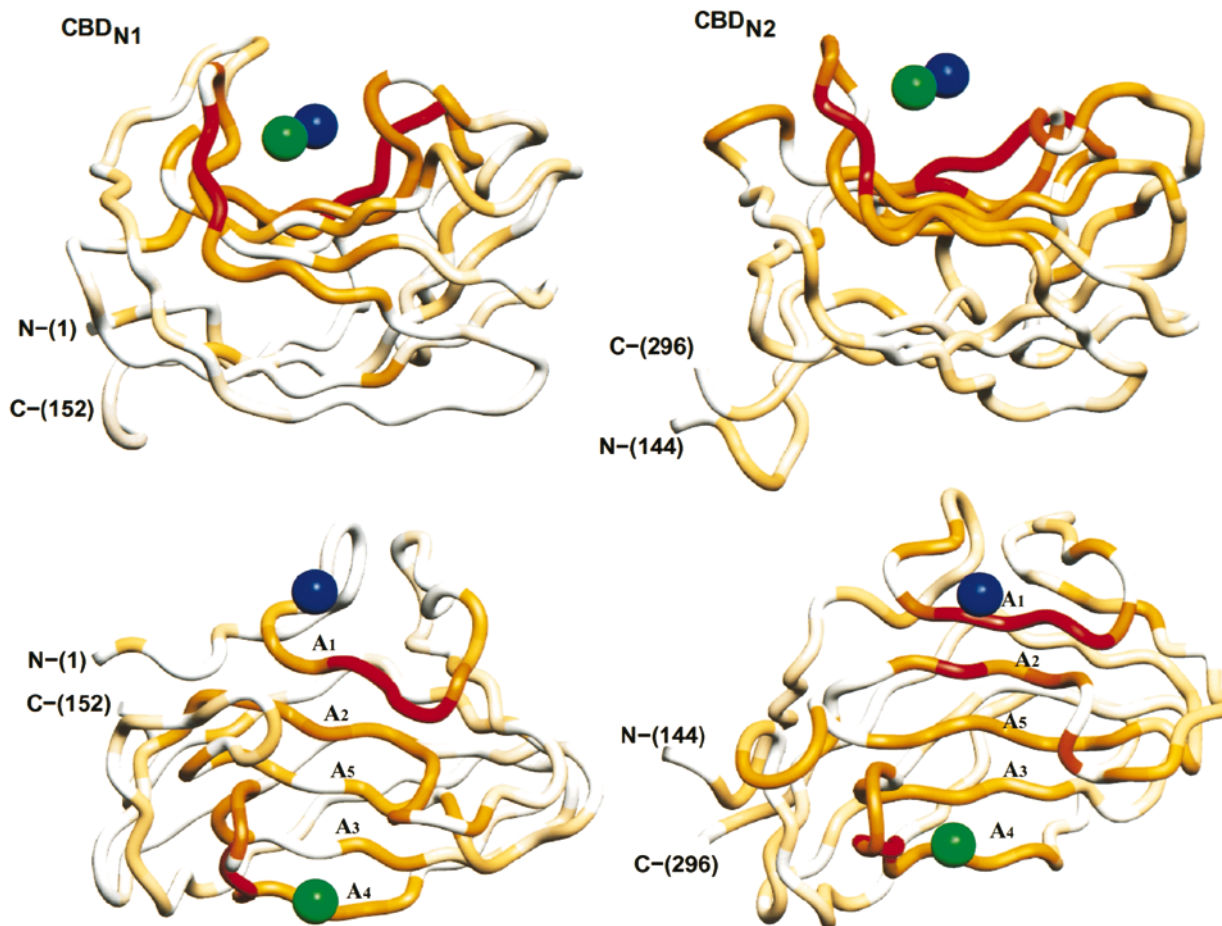heet A in each protein. The individual strands of this β-sheet are labeled. The ribbons are ramp-colored based upon $\Delta R_{2,LW}$ values ranging from 1 Hz (light yellow) to 80 Hz (dark orange). Residues whose $^1H^N$ signals disappear completely in the presence of TEMPO-Glc$_4$ are indicated in red ($\Delta R_{2,LW} > 80$ Hz). The proline residues and other residues for which no results were obtained are shown in white. The green and blue spheres indicate representative positions of the nitroxide groups calculated using an ensemble-averaging protocol in X-PLOR with measured r_{eff} as distance restraints. Note that the TEMPO-Glc$_4$ can occupy only one of these two orientations at any given time.

amides whose relaxation rates were not perturbed significantly by the spin label.

As seen in Figure 4, ΔR_1 and ΔR_2 show similar trends, yet the latter provide a more sensitive indicator of the effects of the spin-labeled sugars on CBD$_{N1}$ and CBD$_{N2}$. In the cases of amide protons with resolved ^1H-^{15}N HSQC cross-peaks that experience moderate paramagnetic relaxation enhancements, the values of $\Delta R_{2,Vol}$ and $\Delta R_{2,LW}$ agree well (ratio = 1.7($\pm$1)). However, a more complete data set could be obtained by measuring changes in line-width rather than volume due to the above mentioned problems associated with dilution effects and difficulties encountered with partially overlapping peaks.

Based on these measurements, it is immediately apparent that amide groups in four regions of CBD$_{N1}$ and four regions of CBD$_{N2}$ experience significant paramagnetic relaxation enhancements due to the bound TEMPO-Glc$_4$. These include

Gly15 to Thr21, Tyr43 to Asn51, Gln80 to Asp90 and Glu122 to Ser133 in CBD$_{N1}$ and Gly160 to Glu172, Trp192 to Asn199, Glu229 to Glu239 and Gly266 to Ala279 in CBD$_{N2}$. These residues lie within the five β-strands, A1 to A5, and adjacent loops that form the cellulose-binding clefts of each protein. Of these four regions, amide protons in strands A1 and A4 that comprise the outer edges of the binding face have markedly larger ΔR_1 and ΔR_2 values than do those in the central strand A5. This verifies that TEMPO-Glc$_4$ binds CBD$_{N1}$ and CBD$_{N2}$ in multiple orientations such that the nitroxide spin label is located at either end of the binding cleft. In contrast, the relaxation rates of amide groups located on the opposite side of each protein relative to this cleft (β-strands B1 to B5) do not exhibit marked enhancements. Similar patterns are observed with TEMPO-Glc$_3$ bound to CBD$_{N1}$ (Supplementary Material).

Calculation of electron-proton distances

Values of τ_c, the correlation time for the fluctuation of the electronic-nuclear dipole-dipole interaction, were calculated for individual residues in both CBD_{N1} and CBD_{N2} bound to TEMPO-Glc$_4$ using the measured ΔR_1 and $\Delta R_{2,Vol}$ or $\Delta R_{2,LW}$ rate enhancements. In the case of CBD_{N1}, τ_c values for 81 amide protons ranged from 0.1 ns to 3.6 ns, with a mean of 1.7($\pm$0.5) ns. For CBD_{N2}, these ranged from 0.1 ns to 6.5 ns for 101 amide protons, with a mean of 1.9($\pm$0.8) ns (Figure 6). The correlation time τ_c is dependent upon both the relaxation of the electron and motions of the electron-proton vector ($1/\tau_c = 1/\tau_S + 1/\tau_R$). In this equation, τ_S is the longitudinal relaxation time of the free electron and τ_R is the effective rotational correlation time of the electron-proton vector. The latter is dependent on the motional characteristics of the protein-ligand complex. Since τ_R is in the range of 10^{-8} to 10^{-9} s for most proteins studied by solution NMR methods, and τ_S is typically longer than 10^{-7} s for nitroxide radicals, τ_c is essentially equal to τ_R (Kosen, 1989). The correlation times for the global tumbling of CBD_{N1} and CBD_{N2} saturated with cellopentaose are approximately 7.4 ns, as determined by ^{15}N relaxation methods (P.E.J., E.B. & L.P.M., unpublished results). The shorter correlation times extracted from the paramagnetic relaxation enhancements may reflect conformational mobility of the bound TEMPO moiety. The large degree of variability in the τ_c values measured for the amide protons in CBD_{N1} and CBD_{N2} is attributed to compounding errors from the ΔR_1 and ΔR_2 measurements, as well as different orientation-dependent effects of internal mobility on the distance between the free electron and the $^1H^N$ of individual amide protons.

Using the τ_c values measured for each residue, the effective electron-proton distances, r_{eff}, between the TEMPO-Glc$_4$ nitroxide and the individual amide protons in CBD_{N1} and CBD_{N2} were calculated. A similar analysis of the data for the TEMPO-Glc$_3$ was not performed due to the occurrence of non-specific relaxation enhancement. The most complete set of relaxation data was obtained from linewidth measurements, and thus the distances reported in Figure 6 were determined using the $\Delta R_{2,LW}$ values; however, similar results were derived from the $\Delta R_{2,Vol}$ rate enhancements. Based on the data in Figure 6, we find that the measured values of r_{eff} range from 11 to 23 Å. Consistent with the previous discussion of the data presented in Figures 2 and 3, the amide protons in CBD_{N1} and CBD_{N2} closest to the nitroxide group are located in β-strands A1 and A4 on the binding faces of the proteins, whereas those that are furthest form strands B1 to B5.

Structure calculations

The positions of the nitroxide moiety in TEMPO-Glc$_4$ bound to CBD_{N1} and CBD_{N2} were calculated using the measured r_{eff} as distance restraints for a simple minimization routine in X-PLOR (Brünger,
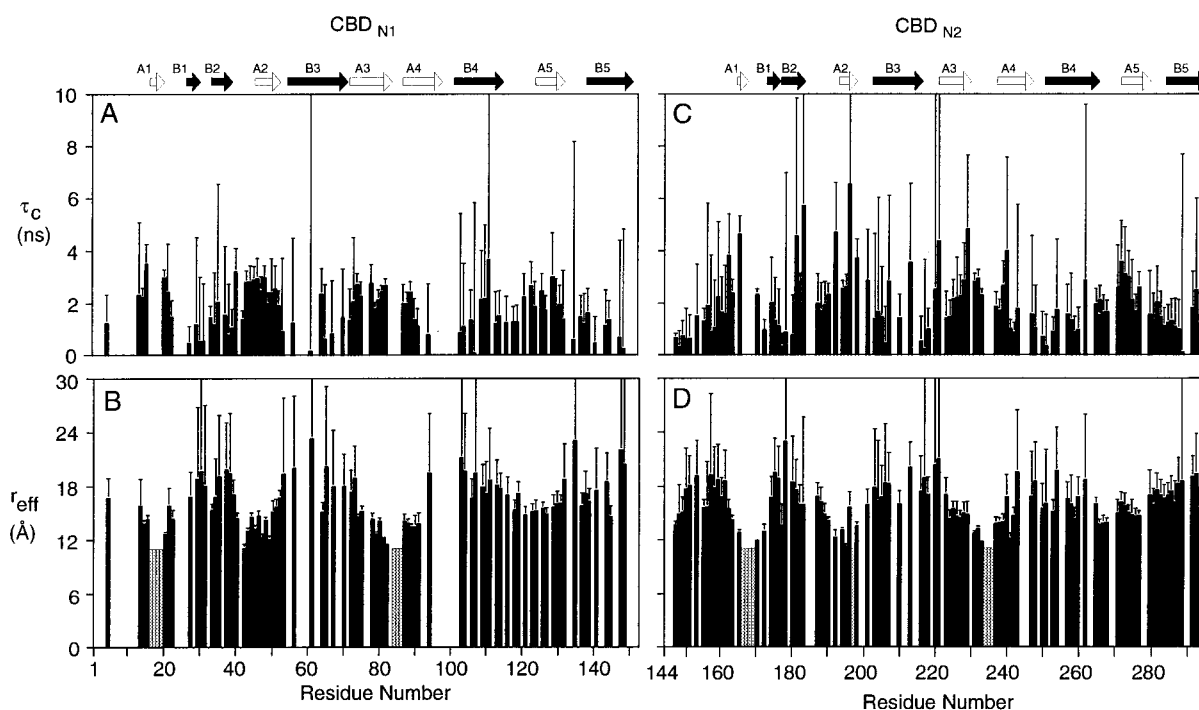
Figure 6. The correlation times, τ_c, and effective electron-proton distances, r_{eff}, calculated for (a), (b) CBD_{N1} and (c), (d) CBD_{N2} bound to TEMPO-Glc$_4$. Residues whose signals disappear completely due to severe linebroadening are shown with a shaded bar at an upper bounds of $r_{eff} = 11$ Å. The locations of the β-strands forming sheets A and B in the two proteins are indicated by the open and filled arrows, respectively.

1992). To account for multiple binding orientations, we used an ensemble-averaging protocol in which $r_{eff} = [1/n \ \Sigma r^{-6}]^{-1/6}$ where r is the electron-proton distance for each of n conformations, assumed to be equally populated (Bonvin & Brünger, 1996). A total of 60 minimization runs were performed using CBD_{N1} or CBD_{N2} in a system with $n = 1, 2,$ or 3 nitroxide groups, modeled as "atoms" of mass 30 amu and a van der Waals radii of 2.5 Å. When only one nitroxide group is utilized, the "atom" is always located in the middle of the binding cleft, approximately above β-strand A5. However, this solution poorly satisfies the experimental restraints requiring the spin label to be closer to amide protons on the edges of the binding cleft than to those near its center. When an ensemble of two nitroxide atoms is considered, we find that in 31/60 and 60/60 cases for CBD_{N1} and CBD_{N2}, respectively, one atom is localized to each edge of the binding cleft (Figure 5). In the remaining 29/60 cases for CBD_{N1}, one atom is found near the middle of the binding cleft and the other distant from the protein. The lowest energies clearly occur in the former situation, with the nitroxide group near β-strands A1 and A4. The difference between the results obtained for the two proteins is attributed to the exact choice of the bounds used for the distance restraints. When an ensemble of three nitroxide atoms is generated, 24/60 and 42/60 cases for CBD_{N1} and CBD_{N2}, respectively, have one atom at each edge of the binding cleft and the third distant from the protein. In the remaining 36/60 and 18/60 cases, the nitroxide groups occupy a variety of positions, close to and distant from the proteins.

Based on these calculations, we conclude that the simplest explanation for the observed patterns of paramagnetic relaxation enhancement is that TEMPO-Glc$_4$ binds both CBD_{N1} and CBD_{N2} in two possible orientations such that the nitroxide moiety lies at either end of the binding cleft (Figure 5). In support of these results, the separation of ∼23 Å between the positions calculated for the nitroxide atoms matches approximately the length of a TEMPO-Glc$_4$ molecule.

Discussion

Binding affinity for spin-labeled cellooligosaccharides

CBD_{N1} and CBD_{N2} bind TEMPO-Glc$_3$ and TEMPO-Glc$_4$ with affinities that are approximately equal to those measured previously for the unmodified sugars. Although the six-membered ring of TEMPO resembles in some ways that of a glucopyranosyl unit, it differs due to the presence of methyl substituents and the absence of equatorial hydroxyl groups. As discussed by Tomme *et al.* (1996a), calorimetric studies have revealed that the binding of soluble cellooligosaccharides to CBD_{N1} is driven by enthalpically favorable interactions such as hydrogen bonding and van der Waals contacts. We therefore conclude that the TEMPO

group does not interact significantly with CBD_{N1} or CBD_{N2} and is positioned in or near the binding cleft solely by virtue of its covalent bonding to the cellooligosaccharides. This statement is supported by the observation that the chemical shift changes accompanying the binding of the modified and unmodified cellooligosaccharides to the two proteins are similar. We also conclude that the presence of an anomeric hydroxyl group does not contribute to the binding of cellooligosaccharides by CBD_{N1} or CBD_{N2}. This is not unexpected given that cellulose, the natural ligand for these proteins, exists in a highly polymeric form.

Multiple binding orientations

Qualitative and quantitative analyses of the effects of TEMPO-Glc$_3$ and TEMPO-Glc$_4$ on the relaxation properties of CBD_{N1} and CBD_{N2} clearly demonstrate that the labeled cellooligosaccharides are bound in at least two orientations. These orientations position the nitroxide moiety at either edge of the binding cleft of each CBD, such that amide protons in β-strands A1 and A4, as well as in the loop between A3 and A4, are perturbed by the spin label to a greater extent that those in the central strand A5 (Figure 5). Since the CBDs form 1:1 complexes with the cellooligosaccharides, these orientations are mutually exclusive such that in any individual CBD complex, the sugar is bound in one direction or the other. Given that the TEMPO-labeled sugars and the corresponding unmodified cellooligosaccharides bind to the CenC CBDs with similar affinities and produce similar chemical shift perturbations, we conclude Glc$_3$, Glc$_4$, and by inference, amorphous cellulose and other soluble β-glucans, are also bound in multiple orientations.

Binding of the unmodified and TEMPO-labeled cellooligosaccharides occurs on an NMR time-scale of fast exchange as evident by the progressive change in the chemical shifts of CBD_{N1} and CBD_{N2} upon the addition of these sugars. Therefore, the chemical shift of an amide proton at any point in the titration reflects a population-weighted average of its chemical shifts in the free and all-bound forms of the CBD. As a result, the equilibrium association constants determined by NMR and calorimetric methods represent apparent or macroscopic K_a values that are the summation of the microscopic binding constants for each possible orientation of the sugar-protein complex (Wyman & Gill, 1990).

An important question to ask is whether a preference for one binding orientation exists. During the titrations of CBD_{N1} and CBD_{N2} with the nitroxide-labeled sugars, it was noted that the signals from residues on β-strand A1 disappeared at lower levels of saturation than did those on A4 (Johnson, 1998). This could indicate that the binding of TEMPO-Glc$_4$ in an orientation with the nitroxide moiety near β-strand A1 is slightly favored, or simply that the nitroxide is positioned closer to the

amides in this strand relative to those in A4. If we assume that the TEMPO-labeled sugars bind in fast exchange between two possible orientations, then the measured r_{eff} is given by:

$$r_{eff} = \left(\frac{f_{b1}}{r_1^6} + \frac{f_{b2}}{r_2^6}\right)^{-1/6}$$

Here r_1 and r_2 are the distances from an amide proton to the two positions of the free electron, and f_{b1} and f_{b2} are the fractions of total protein bound by the ligand in each orientation. Using the positions of the nitroxide atoms shown in Figure 5, we calculate that varying f_{b1} from 0.1 to 0.9 does not change the predicted r_{eff} for amide protons near the edges of the CBD_{N1} and CBD_{N2} binding clefts by more ±20 %. In other words, within experimental error, the effects of any small population differences between the spin-labeled ligands bound in one or the other orientation cannot be distinguished due to the sixth-power dependence of the relaxation enhancement on the proton-electron separation. This is readily seen by considering a case for which $r_1 = 10$ Å and $r_2 = 20$ Å. The calculated r_{eff} is 10.2, 11.2, and 14.4 Å for f_{b1} of 0.9, 0.5, and 0.1, respectively. A similar conclusion was made by Bonvin & Brünger (1995, 1996) when they demonstrated that NOE-derived distances are not sufficient to determine the fractional occupancies of the individual conformations of a protein that exhibits conformational heterogeneity. Because of this limitation, we conservatively estimate that the relative association constants for the binding of TEMPO-Glc$_4$ to CBD_{N1} or CBD_{N2} in the two possible orientations are within a factor of approximately five- to tenfold. Note also that if $r_1 = r_2$ and $f_{b1} = f_{b2}$, then saturation of the CBD at 65 % ($f_{b1} = 0.325$) and 80 % ($f_{b1} = 0.4$) leads to an r_{eff} that is overestimated by only ~7 % and 4 %, respectively.

Extrapolating from these studies, it is reasonable to suggest that TEMPO-Glc$_3$ and TEMPO-Glc$_4$ may be bound in multiple conformations that have one or the other of these two general orientations, yet also differing in the exact position (or register) of the sugar with the β-sheet clefts of CBD_{N1} and CBD_{N2}. Evidence for this hypothesis stems from two observations. First, the longer r_{eff} values (>15 Å) measured in this study, were consistently shorter than the electron-amide proton distances predicted from the calculated positions of the nitroxide atoms shown in Figure 5. Bearing in mind the significant errors associated with the measurement of these distances (see below), this could reflect a small population of ligand shifted to position the nitroxide near the center of the binding clefts of the CBDs and thus transiently close to amide protons in strand A5 and β-sheet B. Second, as noted previously (Johnson et al., 1996a), the $^1H^N$ and ^{15}N chemical shifts of CBD_{N1} and CBD_{N2} are perturbed similarly upon binding of Glc$_3$, Glc$_4$, Glc$_5$, and Glc$_6$. This suggests that the four cellooligosaccharides interact structurally with the CBDs

in the same manner, possibly by sliding within their binding clefts.

Structural symmetry can explain the multiple binding orientations

An explanation for the binding of cellooligosaccharides by CBD_{N1} and CBD_{N2} in multiple orientations is provided by inspection of the structures of both the ligands and the protein molecules. Hydrogen bond formation between the oligosaccharide and the protein provides an enthalpic driving force for binding (Tomme et al., 1996a), and thus the locations of polar atoms within the molecules should be considered. As shown in Figure 7, the hydroxyl and hydroxymethyl groups of cellotetraose are approximately symmetrically disposed such that comparable hydrogen bonds could be formed to the CBDs whether the reducing end of the cellooligosaccharide is located closer to β-strand A1 or A4. In addition, as illustrated in Figure 8, the polar, non-polar, and aromatic side-chains implicated in cellooligosaccharide recognition (Johnson et al., 1996a,b) are approximately symmetrically positioned about the centers of the binding clefts of CBD_{N1} and CBD_{N2}. This provides
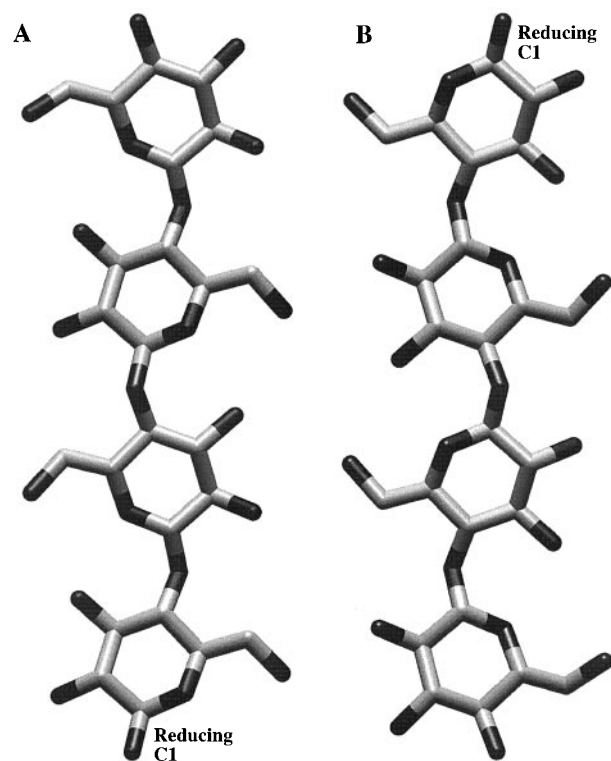
Figure 7. Cellotetraose has approximate symmetry such that its hydroxyl and hydroxymethyl groups would occupy similar positions when the sugar chain is bound in either orientation by CBD_{N1} and CBD_{N2}. (a), (b) Cellotetraose (Geβler et al., 1994) with its reducing end positioned at the bottom or top of the Figure, respectively. The molecules are related by successive 180° rotations about axes perpendicular and parallel to the long axis of the cellooligosaccharide.

Figure 8. The residues implicated in cellulose recognition by the CenC CBDs are positioned approximately symmetrically about the centers of their binding clefts. This may facilitate the binding of a cellooligosaccharide chain i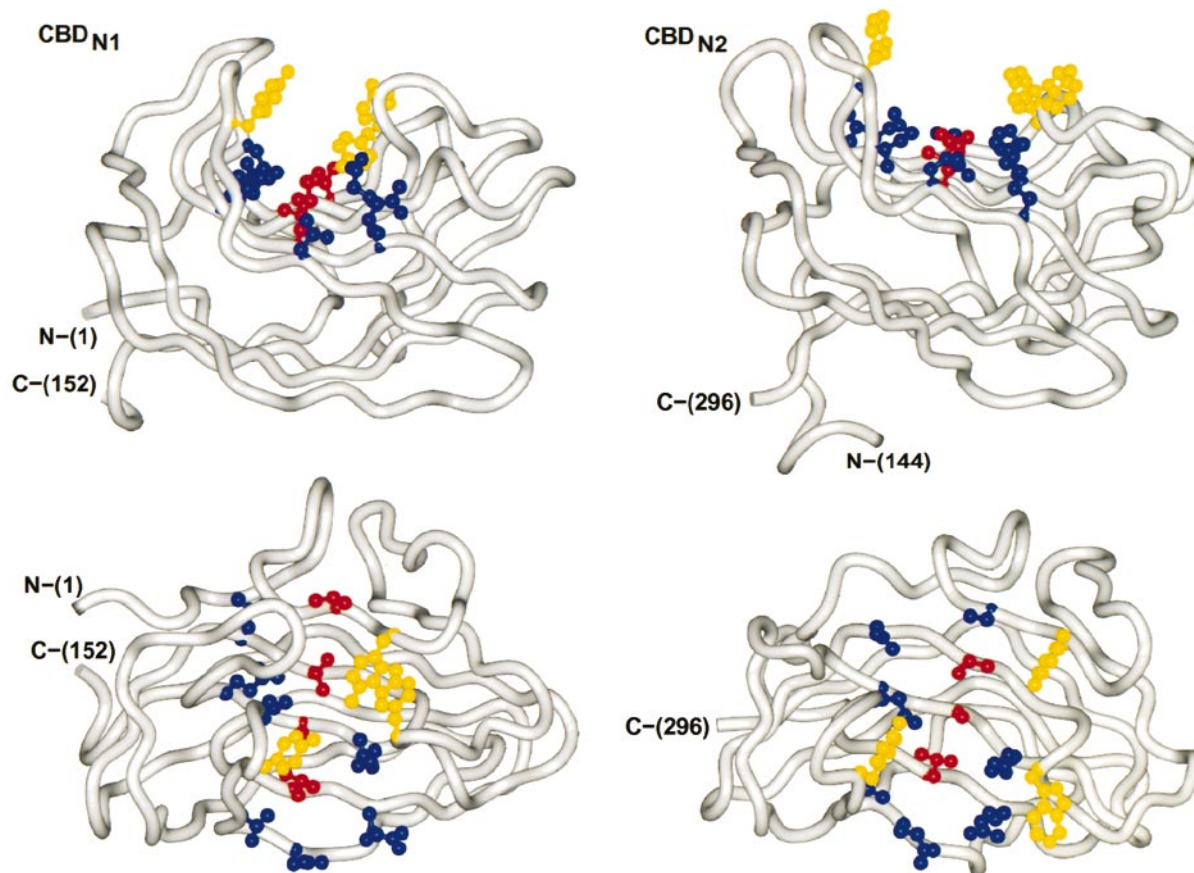n either orientation. Shown are ribbon diagrams of CBD$_{N1}$ (left) and CBD$_{N2}$ (right) positioned for the reader to look across (top) and down onto (bottom) the cellooligosaccharide binding cleft that is formed by β-sheet A in each protein. The side-chains of selected residues within the cellulose binding clefts are color coded as blue, polar; red, hydrophobic; and yellow, aromatic.

further opportunity for the complex formation of the cellooligosaccharides in multiple orientations, while maintaining similar patterns of hydrogen bonds to the equatorial hydroxyl groups and van der Waals contacts to the glucopyranose rings.

It is unlikely that all the oxygen atoms in cellotetraose and the polar atoms in the binding clefts of CBD$_{N1}$ or CBD$_{N2}$ are involved simultaneously in intermolecular hydrogen bonding. The association of cellotetraose with CBD$_{N1}$ involves a $\Delta G°$ of -4.9 kcal mol^{-1} at 35 °C (Tomme *et al.*, 1996a). If the sole contribution to this binding free energy is assumed to be hydrogen bonding involving the 14 sugar hydroxyl groups, each would account for only -0.35 kcal mol^{-1}. Thermodynamic studies of several protein-carbohydrate complexes have demonstrated that the presence of some hydroxyl groups is essential for binding, whereas others are unnecessary or even a hindrance. The net contributions of individual hydroxyl groups to binding generally range from -0.5 kcal mol^{-1} to -2 kcal mol^{-1}, yet can be as high -6 kcal mol^{-1} (Lemieux, 1996; Quiocho, 1993; Street *et al.*, 1986). Based on

these values, CBD$_{N1}$ likely forms between 2.5 and ten hydrogen bonds to cellotetraose. Given the large number of potential hydrogen-bonding sites on this sugar and on the side-chains lining the binding clefts of CBD$_{N1}$ and CBD$_{N2}$, it is reasonable to suggest that cellooligosaccharides, as well as amorphous cellulose, could bind these proteins in many possible conformations with similar free energies. These conformations include opposite orientations of the sugar chain across the β-sheet faces of the CBDs, as well as possible multiple registers within their binding clefts.

Further insights into the binding promiscuity of the CenC CBDs are also gained from dynamic studies of the proteins and protein-sugar complexes using ^{15}N and ^{2}H relaxation measurements. As will be reported elsewhere, the backbone amide protons and methyl-containing side-chains of CBD$_{N1}$ show motional disorder on a nano- to picosecond time-scale that is not restricted upon binding cellopentaose. This internal mobility or flexibility may also allow the cellooligosaccharides to bind in multiple, rapidly interconverting conformations.

Use of spin labels for obtaining ligand-protein distance restraints

Nitroxide-labeled cellooligosaccharides clearly provide a powerful method for characterizing protein-carbohydrate interactions. Qualitatively, the effects of the free radical on the NMR spectra of CBD_{N1} and CBD_{N2} yielded immediate evidence for the binding of TEMPO-Glc_3 and Glc_4 in multiple orientations. Although it was also possible to calculate the effective positions of the nitroxide moiety bound in a minimum of two possible orientations on the CBDs from a quantitative analysis of the measured paramagnetic relaxation enhancement, the accuracy of these models is limited for numerous reasons. These include: (i) complications associated with multiple conformations and partial saturation, as discussed above; (ii) the uncharacterized conformational mobility of the bound TEMPO group; (iii) inaccuracies in the NMR-derived structures of CBD_{N1} and CBD_{N2} calculated without inclusion of the bound Glc_4 or Glc_5, respectively (Johnson et al., 1996b); (iv) errors, which tend to lead to an underestimation of longer values of r_{eff}, arising from difficulties in measuring small values of ΔR_1 and ΔR_2, and from the possibility of relaxation enhancement due to nonspecific binding or to collisions between CBD-TEMPO-Glc_4 complexes in solution; and (v) the lack of distance restraints with $r_{eff} < 11$ Å resulting from the efficiency of paramagnetic relaxation. The latter problem could be addressed by studying CBD_{N1} and CBD_{N2} partially titrated with small quantities of TEMPO-Glc_4 or with mixtures of the labeled sugar in its oxidized and reduced forms in order to identify the amides closest to the bound nitroxide.

To understand in detail the mechanism of cellulose binding by the two Family IV CBDs, we are currently exploiting glycosynthases to prepare selectively ^{13}C-labeled cellooligosaccharides. These compounds will be utilized for isotope-edited and filtered experiments aimed at resolving and assigning intermolecular NOEs between the CBDs and the bound sugars. Using a combination of short-range distance restraints derived from interproton NOE interactions and long-range restraints from electron-proton paramagnetic relaxation enhancements, we hope to define more accurate structural models of the ensembles of the complexes of CBD_{N1} and CBD_{N2} with cellooligosaccharides.

Biological implications

Studies of numerous cellulases and hemicellulases indicate that CBDs facilitate hydrolysis by passively increasing local enzyme concentrations on the surface of cellulosic and hemicellulosic substrates and, possibly, by actively disrupting noncovalent interactions between the chains of these polysaccharides (Tomme et al., 1995). The specificity of CBDs for the various allomorphs of cellulose (e.g. crystalline or amorphous) will also serve

to target these enzymes to distinct regions of this complex substrate.

The results presented here demonstrate clearly that in isolation, CBD_{N1} and CBD_{N2} each bind soluble cellooligosaccharides in multiple orientations. This immediately prompts the question as to the role played by these CBDs within their native context. CenC is a 1069 residue β-1,4-glucanase, composed of CBD_{N1} and CBD_{N2} arranged in tandem at its N terminus, a central family 9 catalytic domain, and two additional domains of unknown function at its C terminus (Coutinho et al., 1992, 1991). The enzyme cleaves a variety of cellulosic substrates and, based on an analysis of its hydrolysis of carboxymethyl-cellulose, is semi-processive with both endo- and exoglucanase activities(Tomme et al., 1996b). Although the structures of the isolated family IV binding domains (CBD_{N1} and CBD_{N2}) and the homologous Family 9 catalytic domains from Clostridium thermocellum celD (Juy et al., 1992) and Thermomonospora fusca E4 (Sakon et al., 1997) have been determined, the spatial arrangement of these modules within native C. fimi CenC remains to be defined.

CBD_{N1} and CBD_{N2} are juxtaposed without an intervening linker. Given that the affinity of the each domain for cellotetraose is equivalent whether joined or in isolation (unpublished), it is likely that CBD_{N1N2} can also bind oligomeric sugars in multiple orientations. This theory is reasonable, as the binding clefts of the two homologous CBDs both span approximately five glycosyl units and thus each domain in CBD_{N1N2} can independently accommodate a single cellooligosaccharide molecule. Preliminary studies indicate that the affinity of CBD_{N1N2} for phosphoric acid swollen cellulose is only approximately 2 fold greater than that of CBD_{N1} for this polymeric substrate (Tomme et al., 1996a). This implies that, when joined in tandem, these CBDs bind amorphous cellulose in an additive, rather than co-operative, manner. A simple interpretation of this result is that the two domains comprising CBD_{N1N2} are structurally constrained, due to the lack of a flexible linker, such that they cannot bind simultaneously to adjacent regions of a single polymer chain. We therefore speculate that the tandem CBDs anchor CenC to its natural substrate by bridging chains of amorphous cellulose without a strong preference for their orientations. Note however, as discussed above, we can only estimate that the relative association constants for the binding of TEMPO-Glc_4 to CBD_{N1} or CBD_{N2} in the two possible orientations are within a factor of approximately five- to tenfold. Thus in combination, CBD_{N1N2} may in fact exhibit a significant overall preference for binding strands of amorphous cellulose positioned to match the yet unknown orientation of the two domains within this tandem CBD. Resolution of this important question hinges upon the determination of the structure of CBD_{N1N2}, as well as further characterization of naturally occurring amorphous cellulose (Bayer et al., 1998).

CBD$_{N1N2}$ is connected to the catalytic domain of CenC by a short proline-rich polypeptide linker sequence (Coutinho *et al.*, 1991, 1992). In contrast to the isolated CBDs, it is certain that this catalytic domain has a definite orientational requirement for the binding and hydrolysis of cellulosic substrates. Although the exact boundaries and thus length of the linker sequence is unknown, the observation that it is highly sensitive to proteolytic cleavage (Tomme *et al.*, 1996b) suggests that the linker affords at least some degree of flexibility between the binding and catalytic domains of CenC. This may allow the cleavage of properly oriented chains of amorphous cellulose other than those to which the CBDs are bound. Processivity would result from the diffusional sliding of both the binding and catalytic domains along the substrate cellulose chains. Enzymatic studies of CenC with and without CBD$_{N1N2}$, as well as structural characterization of the catalytic domain, are clearly necessary to understand the role of these Family IV CBDs in modulating the activity of this *C. fimi* β-1,4-glucanase.

Although over 180 putative CBDs in 13 families have been identified, little is known about the detailed mechanism of cellulose and hemicellulose binding by these protein domains. Studies of several family 2 CBDs, such as those from *C. fimi* Cex, have demonstrated that binding to crystalline cellulose is mediated by conserved aromatic residues aligned along a flat face of the molecule (Xu *et al.*, 1995). Calorimetric measurements have proven that binding is entropically driven(Creagh *et al.*, 1996), indicative of hydrophobic stacking of the aromatic side-chains on the glucose rings. Hydrodynamic studies have also revealed that CBD$_{Cex}$ diffuses readily across the surface of crystalline cellulose (Jervis *et al.*, 1997). We therefore speculate that CBD$_{Cex}$, as well as members of other CBD families, also binds in multiple orientations to cellulose. In contrast, based on the crystal structure of a fragment of the endo/exocellulase E4 containing a family 3c CBD and a family 9 catalytic domain, Sakon *et al.* (1997) have hypothesized that the binding domain aids in the activity of this enzyme by helping to feed a cellulose chain, bound in a defined orientation, into the active site of the catalytic domain. This distinctive behaviour may result from the intimate structural association of the two domains in the *T. fusca* endo/exocellulase.

In summary, we have shown that CBD$_{N1}$ and CBD$_{N2}$ from *C. fimi* CenC bind TEMPO-labeled cellooligosaccharides in multiple orientations. This promiscuous mode of sugar recognition can be attributed to the approximate symmetry of the hydrogen bonding groups on cellulose and on the side-chains lining the binding clefts of these two CBDs. Further structural studies of both native CenC and its substrate, amorphous cellulose, are necessary to understand the mechanisms by which this and other cellulolytic enzymes function in the efficient degradation of biomass.

Materials and Methods

Synthesis of TEMPO-labeled cellooligosaccharides

Details of the synthesis of TEMPO-Glc$_3$ and TEMPO-Glc$_4$ will be provided elsewhere. Ionspray mass spectroscopy of the final products yielded 658 (M+), 659 (M + 1) and 660 (M + 2) for TEMPO-Glc3 (calculated for C$_{27}$H$_{48}$NO$_{17}$: 658.7) and 820 (M+), 821 (M + 1), and 822 (M + 2) for TEMPO-Glc$_4$ (calculated for C$_{33}$H$_{58}$NO$_{22}$: 820.8). Useful ^{1}H-NMR data could not be obtained for these products due to the presence of the spin label. Structural characterization was therefore achieved by reduction of the nitroxide group to a hydroxylamine and acetylation of the entire molecule. The spectral data for these derivatives of TEMPO-Glc$_3$ and TEMPO-Glc$_4$, respectively, are provided below.

2,2,6,6-Tetramethylpiperidin-1-acetoxyl-4-yl 2,3,4,6-tetra-O-acetyl-β-D-glucopyranosyl-(1→4)-2,3,6-tri-O-acetyl-β-D-glucopyranosyl-(1→4)-2,3,6-tri-O-acetyl-β-D-glucopyranoside

^{1}H NMR (500 MHz, CDCl$_3$) δ: 5.14 (dd, 1 H, $J_{3,4}$ 9.6 Hz, H-3), 5.13-5.09 (m, 2 H, H-3' H-3''), 5.05 (dd, 1 H, $J_{4'',5''}$ 9.5 Hz, H-4''), 4.89 (dd, 1 H, $J_{2'',3''}$ 8.8 Hz, $J_{2'',1'}$ 8.1 Hz, H-2''), 4.85 (dd, 1 H, $J_{2',3'}$ 9.5 Hz, $J_{2',1'}$, 8.7 Hz, H-2'), 4.83 (dd, 1 H, $J_{2,3}$ 9.6, Hz $J_{2,1}$ 7.3 Hz, H-2), 4.60-4.47 (m, 4 H, H-1 H-1' H-1'' H6a), 4.42 (dd, 1 H, $J_{6a',6b'}$ 11.7 Hz, $J_{6a',5'}$ 1.5 Hz, H-6a'), 4.34 (dd, 1 H, $J_{6a'',6b''}$ 12.4 Hz, $J_{6a'',5''}$ 4.4 Hz, H-6a''), 4.14 (dd, 1 H, $J_{6b',5'}$ 4.5 Hz, H-6b'), 4.07 (dd, 1 H, $J_{6b,5}$ 5.9 Hz, H-6b), 4.04 (dd, 1 H, $J_{6b'',5''}$ 1.6 Hz, H-6b''), 3.93 (m, 1 H, H-1'''), 3.76 (dd, 1 H, $J_{4',5'}$ 9.4 Hz, H-4'), 3.71 (dd, 1 H, $J_{4,5}$ 9.5 Hz, H-4), 3.65 (m, 1 H, H-5''), 3.63-3.58 (m, 2 H, H-5 H-5'), 2.14-1.98 (33 H, 11 × Ac), 1.83-1.38 (m, 4 H, H-2''' H-3'''), 1.13 (6 H, CH$_3$), 1.10 (6 H, CH$_3$). MS (Ionspray) 1123 (M + 1); calculated for C$_{49}$H$_{71}$NO$_{28}$ (1122.1).

2,2,6,6-Tetramethylpiperidin-1-acetoxyl-4-yl 2,3,4,6-tetra-O-acetyl-β-D-glucopyranosyl-(1→4)- 2,3,6-tri-O-acetyl-β-D-glucopyranosyl-(1→4)- 2,3,6-tri-O-acetyl-β-D-glucopyranosyl -(1→4)- 2,3,6-tri-O-acetyl-β-D-glucopyranoside

^{1}H NMR (400 MHz, CDCl$_3$) δ: 5.15 (dd, 1 H, $J_{3,4}$ 9.5 Hz, H-3), 5.12-5.08 (m, 3 H, H-3' H-3'' H-3'''), 5.04 (dd, 1 H, $J_{4''',5'''}$ 9.5 Hz, H-4'''), 4.89 (dd, 1 H, $J_{2''',3'''}$ 8.9 Hz, $J_{2''',1'''}$ 8.0 Hz, H-2'''), 4.86- 4.81 (m, 3 H, H-2 H-2' H-2''), 4.60-4.47 (m, 5 H, H-1 H-1' H-1'' H-1''' H6a), 4.60-4.32 (m, 3 H, H-6a' H-6a'' H-6a'''), 4.15-4.00 (m, 4 H, H-6b H-6b' H-6b'' H-6b''') 3.95 (m, 1 H, H-1''''), 3.81-3.68 (m, 3 H, H-4 H-4'' H-4'''), 3.66 (m, 1 H, H-5'''), 3.62-3.57 (m, 3 H, H-5 H-5' H-5''), 2.15-1.96 (42 H, 14 x Ac), 1.85-1.37 (m, 4 H, H-2'''' H-3''''), 1.15-1.10 (12 H, 4 × CH$_3$). Ionspray MS 1411 (M + 1); calculated for C$_{61}$H$_{87}$NO$_{36}$ (1410.34).

Protein samples

The ^{15}N-labeled CBD$_{N1}$ (residues 1-152 of CenC) and CBD$_{N2}$ (residues 146-296) were produced by expression of the plasmids pTugN1 and pTugN2 in *Escherichia coli* JM101 cells grown in minimum media containing 1 g/l of ^{15}NH$_4$Cl and 1 g/l of 99 % ^{15}N-labeled Isogro (Isotec Inc.; Johnson *et al.*, 1996a). The secreted proteins were purified from the culture supernatant and the periplasmic fraction using both affinity chromatography on cellulose (Avicel) and ion-exchange chromatography, as

described (Johnson *et al.*, 1996a). Samples of CBD$_{N1}$ and CBD$_{N2}$ were exchanged into a final buffer of 50 mM sodium chloride, 50 mM sodium $^2H_3$-acetate, 3 to 5 mM CaCl$_2$, and 0.02 % sodium azide in 10 % ^2H_2O/90 % H$_2$O at pH* 6.1 using a microsep concentration device (Filtron). CBD$_{N1}$ binds calcium with an equilibrium association constant of $\sim 10^5$ M^{-1} at pH 6.0 and thus exists as a 1:1 CBD$_{N1}$-Ca^{+2} complex under these conditions (Johnson *et al.*, 1998). The metal ion stabilizes the folded structure of CBD$_{N1}$ but does not alter its affinity for cellooligosaccharides. In contrast, CBD$_{N2}$ does not bind calcium appreciably.

Titrations with TEMPO-labeled cellooligosaccharides

The binding of the TEMPO-labeled cellooligosaccharides to the CenC CBDs at pH* 6.1 and 35 °C was measured quantitatively using ^{1}H-^{15}N HSQC spectroscopy. Stock solutions of TEMPO-Glc$_3$ and TEMPO-Glc$_4$ were prepared by weight in the above buffer and added in small aliquots to the protein samples. The titration of CBD$_{N1}$ with TEMPO-Glc$_3$ was carried out by progressively adding the labeled sugar to 0.32 mM protein up to a final ligand-to-protein ratio of 22:1. The titrations of 0.65 mM CBD$_{N1}$ and 0.48 mM CBD$_{N2}$ with TEMPO-Glc$_4$ were taken to final corrected ligand-to-protein ratios of 2.2:1 and 1.4:1, respectively. Protein concentrations were measured using $\varepsilon_{280} = 21370$ M^{-1} cm^{-1} and 20500 M^{-1} cm^{-1} for CBD$_{N1}$ and CBD$_{N2}$, respectively (Johnson *et al.*, 1996a). Equilibrium association binding constants were determined by non-linear least-squares fitting of the ^{1}H^N and ^{15}N chemical shifts of numerous amide protons *versus* cellooligosaccharide concentration to the Langmuir isotherm describing the binding of one ligand molecule to a single protein site(Johnson *et al.*, 1996a). These amide protons, which include Gly7, Gly15, Val34, Gly44, Thr65, Gln80, Asn81, Thr87 and Gly130 for CBD$_{N1}$ and Val197, Tyr198, Gly231, Tyr234 and Ala237 for CBD$_{N2}$, exhibit fast exchange between the free and bound states on the chemical shift time-scale and are detectable, albeit with diminishing intensity, over the course of the entire titration. In the cases of the TEMPO-Glc$_4$ titrations, good fits of the experimental data points to the binding isotherms were obtained only if scaling factors of ~ 1.3 (for CBD$_{N2}$) or 1.8 (for CBD$_{N1}$) were introduced to correct for apparent errors in measuring the weight of the sugar (~ 1 mg) during the preparation of stock titrant solutions. The reported binding constants and errors are the averages and standard deviations of the individual values measured for each ^{1}H^N and ^{15}N nuclei.

NMR spectroscopy

Spectra were acquired on a Varian Unity 500 MHz spectrometer at 35 °C. Each point of the titration of the ^{15}N-labeled proteins with TEMPO-Glc$_3$ or Glc$_4$ was monitored by the acquisition of a sensitivity-enhanced gradient ^{1}H-^{15}N HSQC spectrum (Kay *et al.*, 1992). Upon formation of the sugar-protein complexes, ^{1}H^N T_1 values were measured using a sensitivity-enhanced gradient ^{1}H-^{15}N HSQC sequence as a read-out of a non-selective inversion-recovery experiment recorded with delays of $t = 0, 0.1, 0.2, 0.4, 0.8$ and 2 seconds. The $t = 0.1$ spectrum was repeated to help estimate experimental error. A non-sensitivity-enhanced gradient ^{1}H-^{15}N HSQC spectrum was then recorded to obtain the spin-spin relaxation enhancements, ΔR_2, of the amide ^{1}H^N nuclei. After

completion of the data collection with either CBD$_{N1}$ or CBD$_{N2}$ bound to the paramagnetic cellooligosaccharide, the nitroxide functionality was reduced to the diamagnetic hydroxylamine by the addition of two molar equivalents of solid L-ascorbic acid (Sigma). The pH* of the sample was re-adjusted to 6.1 and the spectra necessary to measure ΔR_1 and ΔR_2 were recorded. All spectra were acquired as 1024×96 complex points with spectral widths of 6500 and 1450 Hz in the ^{1}H and ^{15}N dimensions, respectively. Selective water flip back pulses were utilized to ensure minimum perturbation of the water magnetization (Zhang *et al.*, 1994; Grzesiek & Bax, 1993).

Calculation of ΔR_1 and ΔR_2

NMR spectra were analyzed using a combination of Felix (Biosym Technologies) and NMRPipe (Delaglio *et al.*, 1995). Data for the ^{1}H T_1 series were processed with mild Lorentzian-to-Gaussian apodization. The relative peak volumes, V_t, at each inversion-recovery delay t were fit to the function $V_t = V_o \exp(-t/T_1)$, as described by Farrow *et al.* (1994). V_o is the volume at time $t = 0$, and errors in the measured T_1 lifetimes were estimated using Monte Carlo simulations. The paramagnetic enhancement of each amide proton spin-lattice relaxation rate, ΔR_1, was calculated as:

$$\Delta R_1 = \left(\frac{1}{T_1}\right)_{ox} - \left(\frac{1}{T_1}\right)_{red} \qquad (1)$$

Ox and red indicate the data collected with the labeled cellooligosaccharides in the nitroxide and hydroxylamine forms, respectively.

The non-sensitivity enhanced ^{1}H-^{15}N HSQC spectra were processed without apodization in the proton dimension and with a mild exponential linebroadening window in the nitrogen dimension. Two methods were used to measure individual values of ΔR_2. In the first, the ratio of the peak volumes recorded for an amide in the presence of the nitroxide (V_{ox}) *versus* the hydroxylamine-labeled (V_{red}) cellooligosaccharide is given by:

$$\frac{V_{ox}}{V_{red}} = \frac{e^{-t}/T_{2_{ox}}}{e^{-t}/T_{2_{red}}} \qquad (2)$$

where $t = 10.1$ ms is the total time during the INEPT and reverse-INEPT components of the HSQC pulse sequence in which ^{1}H^N magnetization is in the transverse plane and thus subject to paramagnetic relaxation. A non-gradient enhanced HSQC was utilized to avoid possible complications due to the use of two reverse-INEPT sequences. By measuring total peak volumes, and not heights, the effect of differential T_2 relaxation during the detection periods of the spectra recorded in the presence of the oxidized and reduced sugars can be neglected. Peak volumes were determined by direct integration over a manually adjusted "footprint", and not by fitting of an idealized peak shape. Equation (2) can be rearranged to obtain $\Delta R_{2,vol}$:

$$\Delta R_{2,Vol} = \left(\frac{1}{T_2}\right)_{ox} - \left(\frac{1}{T_2}\right)_{red} = \left(\frac{1}{t}\right)\ln\left(\frac{V_{red}}{V_{ox}}\right) \qquad (3)$$

In the second method, $\Delta R_{2,LW}$ were obtained from the change in the linewidths of the ^{1}H-^{15}N cross-peaks in the proton dimension:

$$\Delta R_{2,LW} = \left(\frac{1}{T_2}\right)_{ox} - \left(\frac{1}{T_2}\right)_{red} = \pi(LW_{ox} - LW_{red}) \qquad (4)$$

where LW_{ox} and LW_{red} are the full half-height line-widths in the presence of the nitroxide and hydroxyla-mine-labeled cellooligosaccharides, respectively. The line-widths were measured by non-linear least-squares fitting of vectors, extracted in the proton dimension through a given cross-peak, to the equation for a single Lorentzian peak split by a $^3J_{HN-H\alpha}$ coupling using the program PLOTDATA (TRIUMPH, UBC, Vancouver, Canada). The coupling constant was either treated as an independent variable or fixed at the value measured previously (Johnson et al., 1996b) using the HNHA or HMQC-J experiments (Bax et al., 1994; Kay & Bax, 1990). Significant errors in the measurement of $\Delta R_{2,LW}$ arise if this coupling is ignored. The effects of the free electron on the relaxation rates of the amide nitrogens are neglected due to the small magnetogyric ratio of the ^{15}N nucleus relative to that of ^1H.

Calculation of r_{eff}

The magnetic interaction of an unpaired electron and a proton is described by the modified Solomon-Bloembergen equations (Solonon & Bloembergen, 1956). The enhancement of the longitudinal (ΔR_1) and transverse (ΔR_2) relaxation rates of a proton due to the spin label are given by the equations (Kosen, 1989; Gellespie & Shortle, 1997a):

$$\Delta R_1 = \Delta\left(\frac{1}{T_1}\right) = \frac{2K}{r^6}\left(\frac{3\tau_c}{1+\omega_H^2\tau_c^2}\right) \qquad (5)$$

$$\Delta R_2 = \Delta\left(\frac{1}{T_2}\right) = \frac{K}{r^6}\left(4\tau_c + \frac{3\tau_c}{(1+\omega_H^2\tau_c^2)}\right) \qquad (6)$$

where K is the constant 1.23×10^{-32} cm^6 s^{-2} for a nitroxide radical, r is the distance between the electron and proton, τ_c is the correlation time for the fluctuation of the electronic-nuclear dipole-dipole interaction, and ω_H is the Larmor frequency of the proton. These equations are based on the assumptions that the vector between the electron and proton is free to undergo isotropic rotational diffusion, and that the distance r is constant. The value of τ_c for each individual amide can be determined directly from the ratio of ΔR_2 to ΔR_1 by combining equations (1) and (2) to obtain:

$$\tau_c = \left(\frac{6\left(\frac{\Delta R_2}{\Delta R_1}\right) - 7}{4\omega_H^2}\right)^{1/2} \qquad (7)$$

With a value of τ_c in hand, the distance between the proton and electron, r, is calculated by rearranging equation (2):

$$r^6 = \frac{K}{\Delta R_2}\left(4\tau_c + \frac{3\tau_c}{(1+\omega_H^2\tau_c^2)}\right) \qquad (8)$$

Individual values of τ_c, rather than a global average, were utilized to reflect directly the experimentally measured relaxation enhancements for each amide. For an ensemble of interconverting protein-ligand complexes, the measured distances will reflect the weighted-average of the individual electron-proton distances and thus are denoted as r_{eff}.

Standard deviations for ΔR_1, ΔR_2, τ_c and r_{eff} were calculated by conventional error propagation (Bevington & Robinson, 1992).

Structure modeling

The positions of the nitroxide moiety in TEMPO-Glc$_4$ bound to CBD$_{N1}$ or CBD$_{N2}$ were estimated using a simple restrained minimization protocol provided with X-PLOR v.3.8 (Brünger, 1992). The only attractive force was the soft-square potential of the distance restraint energy term (E_{NOE}) and the only repulsive force was that corresponding to van der Waals interactions (E_{vdw}). The bounds on the effective electron-proton distances, r_{eff}, were defined for three cases. First, for eight amide protons in CBD$_{N1}$ and eight in CBD$_{N2}$ for which ΔR_2 values could not be obtained due to severe paramagnetic line-broadening (thus $r_{eff} < 11$ Å), the distance bounds were set to the range of 1-11 Å. Second, for 27 amide protons in CBD$_{N1}$ and 26 in CBD$_{N2}$ for which the measured r_{eff} were 11 to 15 Å, the distances were restrained to $r_{eff} \pm 3$ Å. Third, for 54 amides in CBD$_{N1}$ and 59 in CBD$_{N2}$ with $r_{eff} > 15$ Å, the distance bounds were set from 13 Å to an arbitrarily high value of 45 Å. Although distances between 11 and 23 Å were measured for CBD$_{N1}$ and CBD$_{N2}$ (Figure 6), it was found that those >15 Å were consistently underestimated in light of the dimensions of these proteins. Therefore, r_{eff} values greater than 15 Å were used only to derive lower bounds to restrain the nitroxide atoms from approaching the corresponding amide protons in the two protein structures.

To account for multiple positions of TEMPO-Glc$_4$ bound to CBD$_{N1}$ or CBD$_{N2}$, ensemble-averaging (Bonvin & Brünger, 1996) was applied to coordinates systems containing one, two, or three nitroxides, defined as single atoms with a mass of 30 amu and a van der Waal radius of 2.5 Å. The co-ordinates of the protein (pdb file 1ULO for CBD$_{N1}$ and a low-energy structure for CBD$_{N2}$ (unpublished)) were held fixed, and each ensemble of nitroxide groups was minimized 60 times starting from random positions. The quality of the calculated structures were estimated by the NOE energy penalty due to distance restraint violations.

References

Bayer, E. A., Chanzy, H., Lamed, R. & Shoham, Y. (1998). Cellulose, cellulases, and cellulosomes. Curr. Opin. Struct. Biol. 8, 548-557.

Bax, A., Vuister, G. W., Grzesiek, S., Delaglio, F., Wang, A. C., Tschudin, R. & Zhu, G. (1994). Measurement of homo- and heteronuclear J couplings from quantitative J correlation. Methods Enzymol. 239, 79-105.

Bevington, P. R. & Robinson, D. K. (1992). Data Reduction and Error Analysis for the Physical Sciences, 2nd edit., McGraw-Hill Inc., Toronto.

Bonvin, A. M. J. J. & Brünger, A. T. (1995). Conformational variability of solution nuclear magnetic resonance structures. J. Mol. Biol. 250, 80-93.

Bonvin, A. M. J. J. & Brünger, A. T. (1996). Do NMR distances contain enough information to assess the relative populations of multi-conformer structures? *J. Biomol. NMR,* **7**, 72-76.

Brünger, A. (1992). *X-PLOR: A System for X-Ray Crystallography and NMR*, Yale University Press, New Haven.

Cavanagh, J., Fairbrother, W. J., Palmer, A. G. & Skelton, N. J. (1996). *Protein NMR Spectroscopy: Principles and Practice*, Academic Press, Toronto.

Coutinho, J. B., Moser, B., Kilburn, D. G., Warren, R. A. J. & Miller, R. C., Jr. (1991). Nucleotide sequence of the endoglucanase C gene (CenC) of *Cellulomonas fimi*, its high-level expression in *Escherichia coli*, and characterization of its products. *Mol. Microbiol.* **5**, 1221-1233.

Coutinho, J. B., Gilkes, N. R., Warren, R. A. J., Kilburn, D. G. & Miller, R. C., Jr. (1992). The binding of *Cellulomonas fimi* endoglucanase C (CenC) to cellulose and sephadex is mediated by the N-terminal repeats. *Mol. Microbiol.* **6**, 1243-1252.

Creagh, A. L., Ong, E., Jervis, E., Kilburn, D. G. & Haynes, C. A. (1996). Binding of the cellulose-binding domain of exoglucanase Cex from *Cellulomonas fimi* to insoluble microcrystalline cellulose is entropically driven. *Proc. Natl Acad. Sci. USA*, **93**, 12229-12234.

Creagh, A. L., Koska, J., Johnson, P. E., Tomme, P., Joshi, M. D., McIntosh, L. P., Kilburn, D. G. & Haynes, C. A. (1998). Stability and oligosaccharide binding of the N1 cellulose-binding domain of *Cellulomonas fimi* Endoglucanase CenC. *Biochemistry,* **37**, 3529-3537.

Delaglio, F., Grzesiek, S., Vuister, G. W., Zhu, G., Pfeifer, J. & Bax, A. (1995). NMRPipe: a multidimensional spectral processing system based on UNIX pipes. *J. Biomol. NMR,* **6**, 277-293.

Farrow, N. A., Muhandiram, R., Singer, A. U., Pascal, S. M., Kay, C. M., Gish, G., Shoelson, S. E., Pawson, T., Foreman-Kay, J. D. & Kay, L. E. (1994). Backbone dynamics of a free and phosphopeptide-complexed Src homology 2 domain studied by ^{15}N NMR relaxation. *Biochemistry,* **33**, 5984-6003.

Geβler, K., Krauβ, N., Steinr, T., Betzel, C., Sandmann, C. & Saenger, W. (1994). Crystal structure of β-D-cellotetraose hemihydrate with implications for the structure of cellulose II. *Science,* **266**, 1027-1029.

Gellespie, J. R. & Shortle, D. (1997a). Characterization of long-range structure in the danatured state of staphylococcal nuclease. I. Paramagnetic relaxation enhancement by nitroxide spin labels. *J. Mol. Biol.* **268**, 158-169.

Gellespie, J. R. & Shortle, D. (1997b). Characterization of long-range structure in the danatured state of staphylococcal nuclease. II. Distance restraints from paramagnetic relaxation and calculation of an ensemble of structures. *J. Mol. Biol.* **268**, 170-184.

Gnewuch, T. & Sosnovsky, G. (1986). Spin-labeled carbohydrates. *Chem. Rev.* **86**, 203-238.

Grzesiek, S. & Bax, A. (1993). The importance of not saturating H$_2$O in protein NMR. Application to sensitivity enhancement and NOE measurements. *J. Am. Chem. Soc.* **115**, 12593-12594.

Jervis, E. J., Haynes, C. A. & Kilburn, D. G. (1997). Surface diffusion of cellulases and their isolated binding domains on cellulose. *J. Biol. Chem.* **272**, 24016-24048.

Johnson, P. E. (1998). Structural and dynamic analysis of oligosaccharide binding by CBD$_{N1}$. PhD thesis, University of British Columbia, Vancouver, Canada.

Johnson, P. E., Tomme, P., Joshi, M. D. & McIntosh, L. P. (1996a). Interaction of soluble cellooligosaccharides with the N-terminal cellulose-binding domain of *Cellulomonas fimi* CenC. 2. NMR and ultraviolet absorption spectroscopy. *Biochemistry,* **35**, 13895-13906.

Johnson, P. E., Joshi, M. D., Tomme, P., Kilburn, D. G. & McIntosh, L. P. (1996b). Structure of the N-terminal cellolose-binding domain of *Cellulomonas fimi* CenC determined by nuclear magnetic resonance. *Biochemistry,* **35**, 14381-14394.

Johnson, P. E., Creagh, L. A., Brun, E., Joe, K., Tomme, P., Haynes, C. A. & McIntosh, L. P. (1998). Calcium binding by the N-terminal cellulose-binding domains from *Cellulomonas fimi* β-1,4-glucanase CenC. *Biochemistry,* **37**, 12772-12781.

Juy, M., Amit, A. G., Alzari, P. M., Poljak, R. J., Claeyssens, M., Béguin, P. & Aubert, J.-P. (1992). Three-dimensional structure of a thermostable bacterial cellulase. *Nature,* **357**, 89-91.

Kay, L. & Bax, A. (1990). New methods for the measuring of NH-CαH coupling constants in ^{15}N-labelled proteins. *J. Magn. Reson.* **86**, 110-126.

Kay, L., Keifer, P. & Saarinen, T. (1992). Pure absorption gradient enhanced heteronuclear single quantum correlation spectroscopy with improved sensitivity. *J. Am. Chem. Soc.* **114**, 10663-10665.

Kleerekoper, Q., Howarth, J. W., Guo, X., Solaro, R. J. & Rosevear, P. R. (1995). Cardiac troponin I induced conformational changes in cardiac troponin C as monitored by NMR using site-directed spin and isotope labeling. *Biochemistry,* **34**, 13343-13352.

Kosen, P. A. (1989). Spin labeling of proteins. *Methods Enzymol.* **177**, 86-121.

Lemieux, R. U. (1996). How water provides the impetus for molecular recognition in aqueous solution. *Acc. Chem. Res.* **29**, 373-380.

Mackenzie, L. F., Wang, Q., Warren, R. A. J. & Withers, S. G. (1998). Glycosynthases: mutant glycosidases for oligosaccharide synthesis. *J. Am. Chem. Soc.* **120**, 5583-5584.

Otting, G. & Wüthrich, K. (1990). Heteronuclear filters in two-dimensional [^{1}H,^{1}H]-NMR spectroscopy: combined use with isotope labelling for studies of macromolecular conformation and intermolecular interactions. *Quart. Rev. Biophys.* **23**, 39-96.

Plessas, N. R. & Goldstein, I. J. (1981). Synthesis of α- and β-glycosides containing spin labels as probes for studies of carbohydrate-protein interactions. *Carbohydrate Res.* **89**, 211-220.

Quiocho, F. (1989). Protein-carbohydrate interactions: basic molecular features. *Pure Appl. Chem.* **61**, 1293-1306.

Quiocho, F. A. (1993). Probing the atomic interactions between proteins and carbohydrates. *Biochem. Soc. Trans.* **21**, 442-448.

Sakon, J., Irwin, D., Wilson, D. B. & Karplus, P. A. (1997). Structure and mechanism of endo/exocellulase E4 from Thermonospora fusca. *Nature Struct. Biol.* **4**, 810-818.

Solomon, L. & Bloembergen, N. (1956). Nuclear magnetic interactions in the HF molecule. *J. Chem. Phys.* **25**, 261-266.

Street, I. P., Armstrong, C. R. & Withers, S. G. (1986). Hydrogen bonding and specificity. Fluorodeoxy sugars as probes of hydrogen bonding in the glyco-

gen phosphorylase/glucose complex. *Biochemistry,* **25**, 6021-6027.

Tomme, P., Warren, R. A. J., Miller, R. C., Jr, Kilburn, D. G. & Gilkes, N. R. (1995). Cellulose-binding domains: classification and properties. In *Enzymatic Degradation of Insoluble Polysaccharides* (Saddler, J. N. & Penner, M., eds), pp. 142-161, American Chemical Society, Washington, DC.

Tomme, P., Creagh, A. L., Kilburn, D. G. & Haynes, C. A. (1996a). Interaction of polysaccharides with the N-terminal cellulose-binding domain of *Cellulomonas fimi* CenC. 1. Binding specificity and calorimetric analysis. *Biochemistry,* **35**, 13885-13894.

Tomme, P., Kwan, E., Gilkes, N. R., Kilburn, D. G. & Warren, R. A. J. (1996b). Characterization of CenC, an enzyme from *Cellulomonas fimi* with both endo- and exoglucanase activities. *J. Bacteriol.* **178**, 4216-4223.

Vyas, N. K. (1991). Atomic features of protein-carbohydrate interactions. *Curr. Opin. Struct. Biol.* **1**, 732-740.

Wyman, J. & Gill, S. J. (1990). *Binding and Linkage. Functional Chemistry of Biological Macromolecules*, University Science Books, Mill Valley.

Xu, G.-Y., Ong, E., Gilkes, N. R., Kilburn, D. G., Muhandiram, D. R., Harris-Brandts, M., Carver, J. P., Kay, L. E. & Harvey, T. S. (1995). Solution structure of a cellulose-binding domain from *Cellulomonas fimi* by nuclear magnetic resonance spectroscopy. *Biochemistry,* **34**, 6993-7009.

Yu, L., Meadows, R. P., Wagner, R. & Fesik, S. W. (1994). NMR studies of the FK506 binding protein bound to a spin-labeled ascomycin analog. *J. Magn. Reson.* **104**, 77-80.

Zhang, O., Kay, L. E., Olivier, J. P. & Foreman-Kay, J. D. (1994). Backbone ^{1}H and ^{15}N resonance assignments of the N-terminal SH3 domains of drk in folded and unfolded states using enhanced-sensitivity pulsed field gradient NMR techniques. *J. Biomol. NMR,* **4**, 845-858.

Zhao, Q., Abeygunawardana, C. & Mildevan, A. S. (1997). NMR studies of the secondary structure in solution and the steroid binding site of delta5-3-ketosteroid isomerase in complexes with diamagnetic and paramagnetic steroids. *Biochemistry,* **36**, 3458-3472.

Edited by P. E. Wright

JMB Online

http://www.academicpress.com/jmb

Supplementary material comprising one Figure is available from JMB Online